Journal of Biomolecular NMR, 5 (1995) 97–102
ESCOM

J-Bio NMR 238

A simultaneous $^{15}N,^{1}H$- and $^{13}C,^{1}H$-HSQC with sensitivity enhancement and a heteronuclear gradient echo

M. Sattler, M. Maurer, J. Schleucher* and C. Griesinger**

Institut für Organische Chemie, Universität Frankfurt, Marie Curie Strasse 11, D-60439 Frankfurt, Germany

Received 19 August 1994
Accepted 13 October 1994

Keywords: B_0-gradients; COS-CT; COS-INEPT; Heteronuclear NMR; Sensitivity enhancement; Simultaneous COS-INEPT; Simultaneous HSQC; Solvent suppression

Summary

New pulse sequences are introduced and discussed that allow for simultaneous acquisition of $^{15}N,^{1}H$- and $^{13}C,^{1}H$-HSQC correlations for fully $^{13}C,^{15}N$-labeled biomacromolecules in combination with heteronuclear gradient echoes and sensitivity enhancement. The pulse sequence experimentally found to be optimal can be used as a building block, especially in time-consuming multidimensional NMR experiments. Due to the excellent solvent suppression obtained by employing heteronuclear gradient echoes, which allows detection of resonances under the water resonance, it would be possible to record two sensitivity-enhanced 4D experiments simultaneously on one sample dissolved in H_2O, e.g. a 4D $^{13}C,^{1}H$-HSQC-NOESY-$^{15}N,^{1}H/^{13}C,^{1}H$-HSQC.

In NMR spectroscopy of biomacromolecules it is desirable to record all experiments on a single sample dissolved in H_2O, in order to reduce the number of samples and at the same time increase the comparability of spectra. This is even more essential for costly isotopically labeled samples. For such samples excellent suppression of water and artifacts, e.g. t_1 noise, can be achieved in heteronuclear experiments (Hurd and John, 1991) that make use of heteronuclear gradient echoes (Maudsley et al., 1978).

Implementations of heteronuclear correlation experiments with and without application of a heteronuclear gradient echo differ in the type of coherence selected during the evolution time (Schleucher et al., 1993). While the Cartesian operators of the type I_x, I_y that lead to an amplitude-modulated signal are selected in alternating transients in conventional experiments without the application of gradients, the application of a gradient echo necessarily implies that the operators I^+ or I^- are selected, yielding a phase-modulated signal. Whether I^+ or I^- is selected depends on the relative amplitude of the gradients causing the heteronuclear gradient echo. Echo and antiecho data yield spectra with pure phases by appropriate processing (Palmer et al., 1991). However, the pulse sequences that transfer Cartesian operators (amplitude-modulating pulse sequences) yield reduced sensitivity when heteronuclear gradient echoes are incorporated. By contrast, when pulse sequences are used that transfer spin operators of the type I^+ or I^- to I^-, and thus yield a coherence order-selective transfer, no loss in sensitivity occurs upon formation of a heteronuclear gradient echo (Kay et al., 1992; Schleucher et al., 1993). Therefore, sequences that transfer **C**oherence **O**rders in a **S**elective (COS-coherence transfer) way (Palmer et al., 1991; Kay et al., 1992; Muhandiram et al., 1993; Schleucher et al., 1993,1994; Muhandiram and Kay, 1994) are highly desirable because introduction of gradients does not lead to a loss in signal-to-noise. In the first implementation of this principle (Palmer et al., 1991; Kay et al., 1992; Schleucher et al., 1993) (Fig. 1a), X→H transfer is achieved by a COS-INEPT step. In this experiment, sensitivity enhancement of a factor $\sqrt{2}$ can be achieved for the transfer of antiphase heteronuclear coherence $2F_zS^-$ to F^- ($F^- = \sum_i^n I_i^-$) in IS spin systems, compared to conventional pulse sequences. Roughly equal sensitivity can be obtained for I_2S and I_3S spin systems (Schleucher et al., 1994).

*Current address: Dept. of Biochemistry, University of Wisconsin-Madison, 420 Henry Mall, Madison, WI 53706, U.S.A.
**To whom correspondence should be addressed.

a

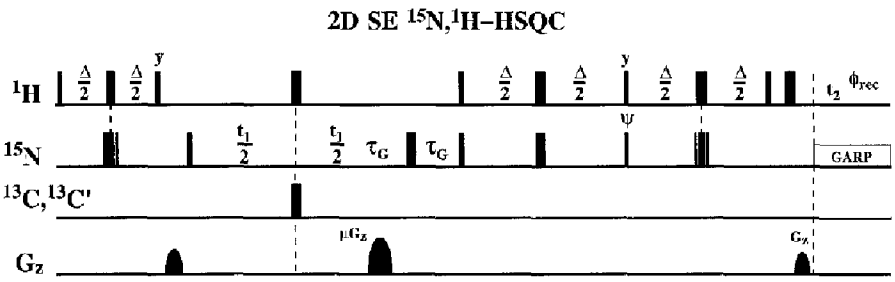

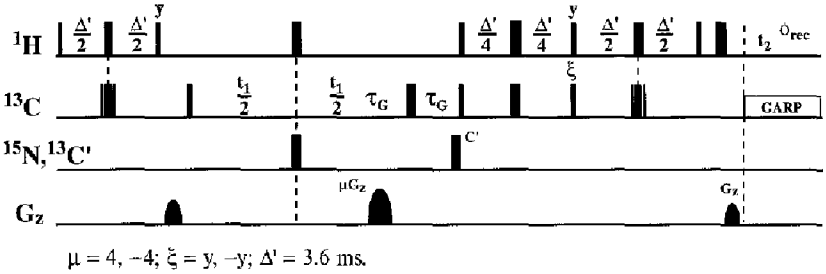

b

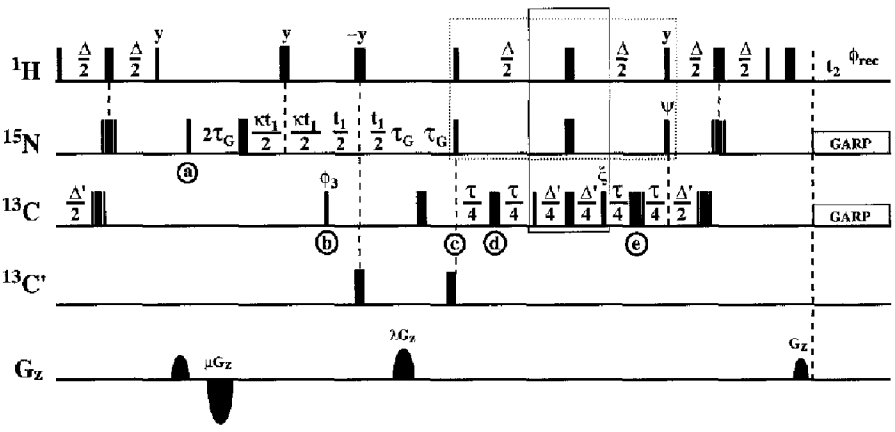

Fig. 1. (a) Sensitivity-enhanced ^{15}N,^{1}H-HSQC and ^{13}C,^{1}H-HSQC with COS-INEPT for the X→H transfer. $\Delta = 1/2J_{NH}$ and $\Delta' = 1/2J_{CH}$. The first gradient is a homospoil gradient, the second (μG_z) effects coherence order selection. Note the different phases $\psi = -y$ and $\xi = y$, due to the different sign of the gyromagnetic ratios of ^{15}N and ^{13}C. All pulse phases are x, unless indicated otherwise. Composite pulses (90°_y, 180°_x, 90°_y) are used for the inversion of z-magnetization of the ^{13}C and ^{15}N spins. (b–d) Three different possible implementations of simultaneous sensitivity-enhanced ^{15}N,^{1}H- and ^{13}C,^{1}H-HSQC with COS-CT. In all sequences longitudinal two-spin order $2F_zS_z$ ($F^- = \sum_i^n I_i^-$) for ^{1}H and ^{13}C is stored at the beginning of the evolution time (point a) to allow for the longer t_1 increment of nitrogen, $(1 + \kappa)\,\Delta t_1$, compared to that of carbon (Δt_1). The gradients applied lead to equal dephasing of carbon and nitrogen coherence after the evolution time, as explained in the text. (b) The initial part of the COS-INEPT (box with dashed line) for the ^{1}H-^{15}N systems is identical to the sequence in Fig. 1a. The first three carbon pulses (solid box) of the COS-INEPT for the ^{1}H-^{13}C systems are positioned centrosymmetrically in the middle of the equivalent pulses for the ^{1}H-^{15}N systems. The two 180°(^{13}C) pulses at positions d and e serve to refocus the $^{1}J_{C,H}$ couplings during τ/2. (c) Compared to the sequence in (b), the refocussing of $^{1}J_{C,H}$ during τ/2 is now achieved by two pairs of 180°(^{1}H,^{15}N) pulses at positions d and e. The sequence in Fig. 1b suffers from the evolution of $^{1}J_{^{13}C,^{13}C}$ couplings for $t_1 = 0$ and the large number of pulses that have to be applied compared to the reference experiments in (a). (d) This sequence is recommended. It avoids the evolution of C,C coupling to a large extent by positioning the first three carbon pulses of the ^{13}C,^{1}H-COS-INEPT (solid box) at the beginning of the first pulses of the ^{15}N,^{1}H-COS-INEPT. Compared to (a), only one pair of 180°(^{1}H,^{15}N) pulses has to be applied additionally. This sequence and the sequence of (b) were used to record the simultaneous ^{15}N,^{1}H- and ^{13}C,^{1}H-HSQC shown in Fig. 2. (e) Reduction of the COS-INEPT parts of the sequence in (d) to either of the sequences in (a). For the ^{15}N→^{1}H transfer, the 180°(^{1}H,^{15}N) pulse pair can be shifted to the left. The first 180°_x(^{15}N) pulse commutes with the first 90°_y(^{15}N) pulse. The 180°(^{1}H) pulse is merged with the first 90°(^{1}H) pulse, yielding a 90°_x(^{1}H) pulse. Since the sign of this pulse phase is irrelevant for the coherence selected, the reduced sequence on the right can be regarded as identical with the sequence in (a). For the ^{13}C→^{1}H transfer (lower part sequences), the delay Δ–Δ'/2 (crossed out) can be omitted since no heteronuclear coupling evolves. The hatched 180°(^{1}H) pulse can be shifted to the left through the delay Δ'/2, requiring a sign change in one of the gradients or a 180° phase change in, for example, the second 90°(^{13}C) pulse. Since the sign of the phase of the first 90°(^{1}H) pulse is irrelevant, the sequence on the right can be regarded as identical to the one in (a).

c

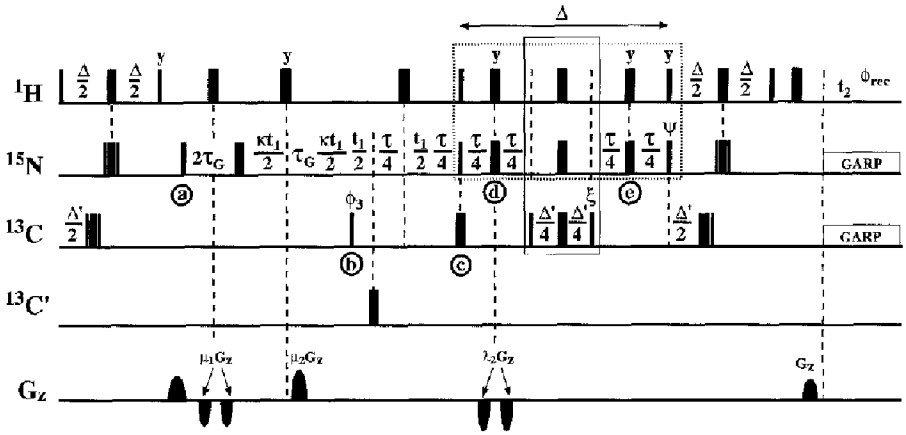

$\mu_1 = -4, 4; \mu_2 = 2, -2; \lambda_2 = -2, 2; \psi = y, -y; \xi = -y, y;$
$\Delta = 5.4$ ms; $\Delta' = 3.6$ ms; $\tau_G = 1.8$ ms $= \tau/2 = (\Delta/2 - \Delta'/4)$.

d

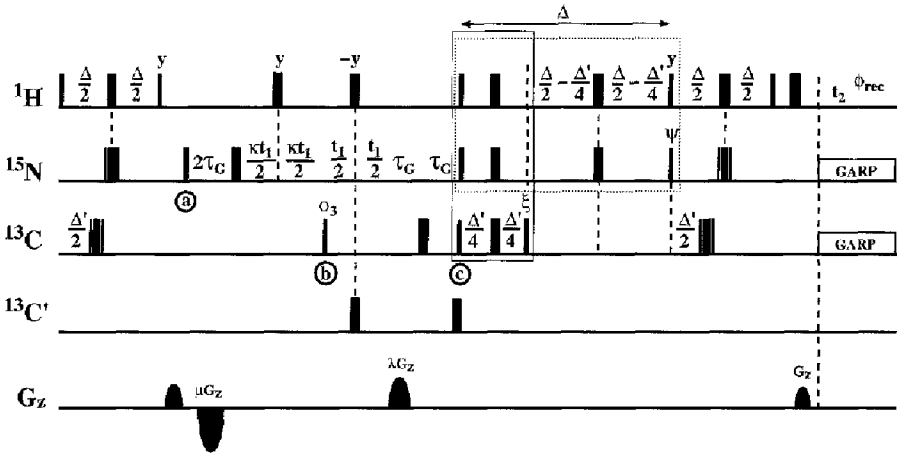

$\mu = -6, 6; \lambda = 4, -4; \psi = -y, y; \xi = -y, y;$
$\Delta = 5.4$ ms; $\Delta' = 3.6$ ms; $\tau_G = 1.8$ ms.

e

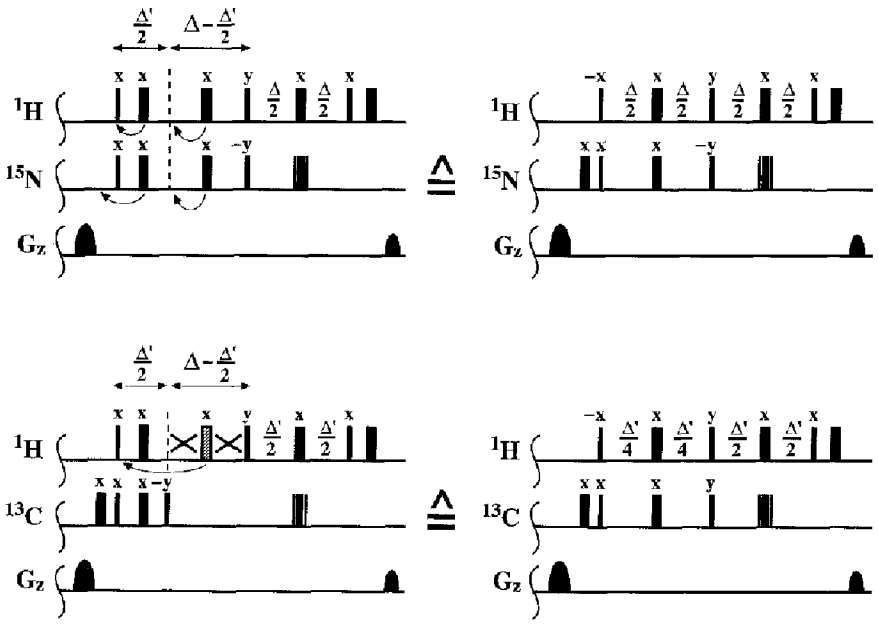

Fig. 1. (continued).

In addition, sensitivity obtained for a given experiment time can be enhanced by simultaneous acquisition of e.g. ^{15}N,^{1}H- and ^{13}C,^{1}H-correlations in heteronuclear correlation experiments which contain as a final step an HSQC-like transfer from heteronuclear coherence to proton coherence (Sørensen, 1990; Farmer, 1991; Boelens et al., 1994; Mariani et al., 1994). The application of simultaneous experiments is highly desirable for the most time-consuming experiments, i.e., 4D HSQC-NOESY-HSQC (Ikura et al., 1990; Clore et al., 1991; Zuiderweg et al., 1991) and has been shown to be feasible for a 3D NOESY-HSQC experiment (Pascal et al., 1994). Simultaneous $^{13}C\rightarrow^{1}H$ and $^{15}N\rightarrow^{1}H$ correlation has also been used in a simultaneous H(X)YH correlation experiment (Mariani, 1994). Simultaneous ^{15}N-^{1}H and ^{13}C-^{1}H excitation has been used for 4D HSQC-NOESY-HSQC by Farmer and Mueller (1994).

In this communication, we introduce a building block that allows sensitivity-enhanced simultaneous ^{13}C-^{1}H and ^{15}N-^{1}H detection and is compatible with the use of a heteronuclear gradient echo for water suppression. The rationales behind the design of the pulse sequence are the following. First, the pulse sequence should meet the requirement that the chemical shift region of the carbons must have a smaller t_1 increment than that of nitrogen. Second, the different size of the heteronuclear coupling constants $^{1}J_{N,H}$ and $^{1}J_{C,H}$ should also be taken into account during defocussing and refocussing. And third, all proton magnetization should pass the final B_0-gradient applied to protons before detection. Therefore, transverse nitrogen magnetization must be subjected to a 2.5 times stronger gradient than transverse carbon magnetization. This requires application of gradients during delays in the sequence where nitrogen and carbon magnetization have different coherence orders. Three pulse sequences that meet these requirements and have been experimentally tested are shown in Figs. 1b–d and are discussed in the following.

Due to the smaller spectral width of nitrogen compared to carbon, the chemical shift evolution of nitrogen with an increment of $(1 + \kappa)\ \Delta t_1$ starts earlier in all sequences (point a) than that of carbon (point b) with an increment Δt_1 in the sequences of Figs. 1b–d. Carbon magnetization is stored as $2F_zS_z$ (where F refers to the proton and S to the carbon spin) between points a and b in all pulse sequences (Figs. 1b–d), while nitrogen magnetization is transverse already. In Figs. 1b and d, B_0-gradients μG_z ($\mu = \mp 6$) are applied during that time and the nitrogen magnetization is dephased with $\mp 6\ G_z\ \gamma_N$. In the pulse sequence of Fig. 1c the gradients of amplitude $2\mu_1 G_z$ ($\mu_1 = \mp 4$) and $\mu_2 G_z$ ($\mu_2 = \mp 2$) already yield dephasing of the transverse nitrogen magnetization by $(2\mu_1-\mu_2)\ G_z\ \gamma_N = \mp 10\ G_z\ \gamma_N$. (Note that a 180° pulse inverts the coherence order of magnetization, so that gradients applied before and after a 180° pulse must have different signs to be additive.) Then the carbon magnetization is also turned into the transverse plane (point b in Figs. 1b–d) and a gradient λG_z ($\lambda = \pm 4$) in the sequences of Figs. 1b and d and two gradients $\lambda_2 G_z$ ($\lambda_2 = \mp 2$) in the sequence of Fig. 1c are applied that dephase transverse carbon magnetization by $\pm 4\ G_z\ \gamma_C$. In the sequences of Figs. 1b and d, the gradient λG_z also yields a dephasing of the transverse nitrogen magnetization by $\mp 4\ G_z\ \gamma_N$, which adds to the phase $\mp 6\ G_z\ \gamma_N$, acquired between points a and b. By contrast, in the sequence of Fig. 1c no dephasing of nitrogen magnetization is effected by the two gradients $\lambda_2 G_z$, due to the refocussing 180°(^{15}N) pulse at point d. At this point, nitrogen ($\mp 10\ G_z\ \gamma_N$) and carbon ($\pm 4\ G_z\ \gamma_C$) have acquired identical dephasing in the sequences of Figs. 1b–d, due to the B_0-gradients, since $\gamma_{13_C}/\gamma_{15_N} = -2.5$. Note that the coherence orders of nitrogen and carbon magnetization are different in sign because of the negative sign of the ratio of $\gamma_{13_C}/\gamma_{15_N}$. The 180° pulses on either proton, carbon or nitrogen between points a and c ensure that neither $^{1}J_{C,H}$ nor $^{1}J_{N,H}$ couplings evolve during t_1 and that chemical shifts for carbon and nitrogen are refocussed for $t_1 = 0$.

The most important differences between the three sequences (Figs. 1b–d) are found for the $^{15}N\rightarrow^{1}H$ and $^{13}C\rightarrow^{1}H$ COS-INEPT. Since the proton pulses affect the protons bound to carbon as well as those bound to nitrogen, they must be used for both proton species. In the first (Fig. 1b) and second implementation (Fig. 1c), the N→H transfer is essentially unchanged compared to Fig. 1a, except for additional 180°(H,N) pulses in the dotted box (Fig. 1c) which, however, do not change the evolution of any interaction compared to the ^{15}N,^{1}H-HSQC employing COS-INEPT (Fig. 1a, upper half). For sequences in Figs. 1b and c the carbon pulses in the solid box are placed symmetrically in the middle of the nitrogen pulses in the dotted box. Carbon and proton/nitrogen π pulses, respectively, are placed in the sequences of Figs. 1b and c in such a way that the $^{1}J_{H,N}$ coupling evolves during $1/2\,^{1}J_{H,N}$ and the $^{1}J_{H,C}$ coupling during $1/4\,^{1}J_{H,C}$. The disadvantage of the implementation in Fig. 1b is the prolonged time during which the $^{1}J_{13_C,13_C}$ couplings evolve compared to the reference experiment in Fig. 1a, namely $\tau/2 = 1.8$ ms. In addition, more pulses have to be applied on either ^{13}C (Fig. 1b) or ^{1}H and ^{15}N (Fig. 1c). The implementation in Fig. 1d, which puts the first three carbon pulses (solid box) asymmetrically at the beginning of the first delay $\Delta = 1/2\,^{1}J_{H,N}$, solves both problems. No transverse carbon magnetization is left after the 90°(^{13}C) pulse with phase ξ. For $t_1 = 0$ the $^{1}J_{13_C,13_C}$ couplings evolve during $2\tau_C$ and also during $\Delta'/2$ for one of the Cartesian magnetization components, which is identical to the reference experiment. Only one additional pair of 180°-(^{1}H,^{15}N) pulses is needed for the simultaneous COS-INEPT of Fig. 1d compared to the COS-INEPT parts of the reference experiments (Fig. 1a).

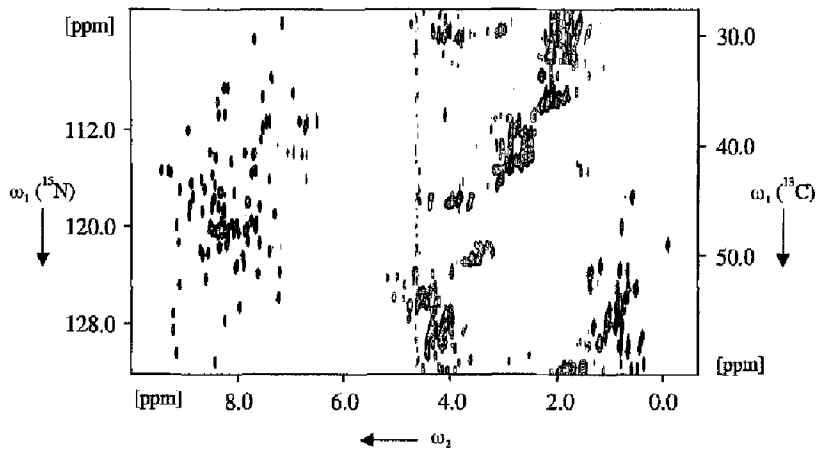

Fig. 2. Simultaneous sensitivity-enhanced $^{15}N,^{1}H$- and $^{13}C,^{1}H$-HSQC of a 2 mM sample of completely ^{13}C- and ^{15}N-labeled rhodniin, a 103-residue protein, in a Shigemi tube. κ was set to 1.77 and the t_1 increment Δt_1 to 200 μs, yielding spectral widths of 1805 Hz for ^{15}N and 5000 Hz for ^{13}C, resulting in folding of the aliphatic carbons. The figure shows correlations between $^{15}N,^{1}H$ and aliphatic $^{13}C,^{1}H$. Note the excellent water suppression that allows observation of the H^{α} resonances even under the water resonance.

Some remarks should be made regarding the signs of the pulse phases (ψ, ξ) and gradients in the different sequences. The COS-INEPT part (after the evolution time) of the pulse sequences in Fig. 1a accomplishes an effective Hamiltonian for an IS spin system: $2\pi J(I_xS_x + I_yS_y)$ with $\psi = -90°$. This Hamiltonian leads to an anti-echo transfer. Inverting the sign of either of the two 90°(S) pulses or of either of the second or third 90°(I) pulses, the effective Hamiltonian is: $2\pi J(I_xS_x - I_yS_y)$ (ψ = 90°), which leads to an echo transfer and therefore requires opposite gradient signs compared to the anti-echo transfer. Taking the sequences in Fig. 1a as a reference, rules are provided that allow reduction of any of the sequences in Figs. 1b–d to those in Fig. 1a. If we ignore the chemical shift evolution that is refocussed by the 180° pulses, then (i) a pair of 180°(I,S) pulses can be shifted until a 90° pulse is reached, because the heteronuclear coupling Hamiltonian $2\pi J I_zS_z$ commutes with the

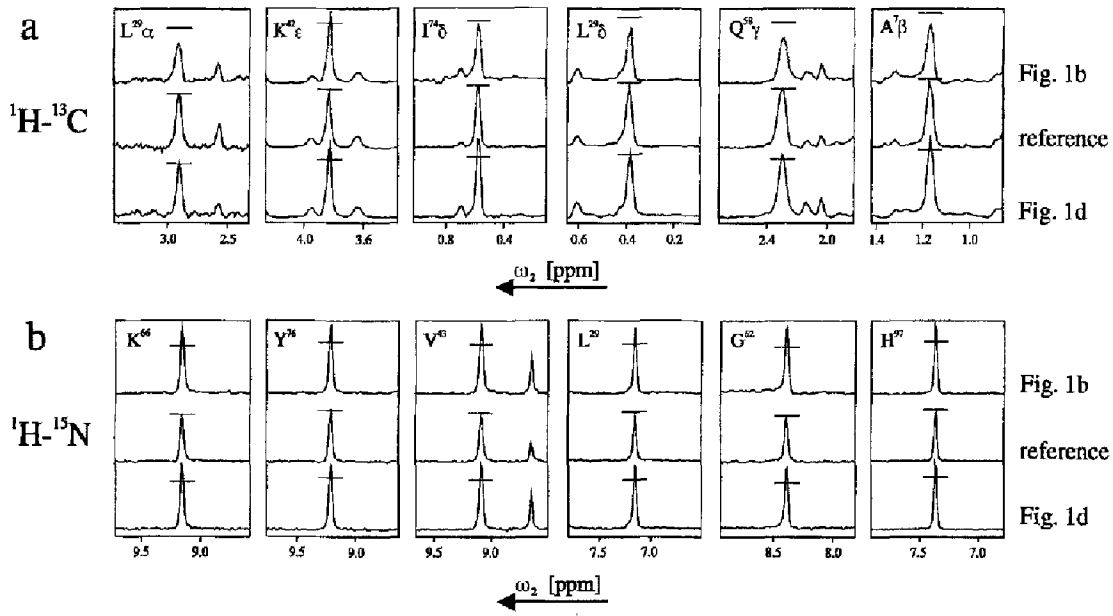

Fig. 3. Representative traces through the simultaneous $^{15}N,^{1}H$- and $^{13}C,^{1}H$-HSQC recorded in 1.5 h with the optimized pulse sequence of Fig. 1d (bottom) and with the less sensitive pulse sequence of Fig. 1b (top). The middle trace was obtained from a $^{13}C,^{1}H$-HSQC with a COS-INEPT transfer (Fig. 1a, lower half) with $\Delta' = 1/2J_{CH}$ (for Fig. 3a) and from a $^{15}N,^{1}H$-HSQC with a COS-INEPT transfer (Fig. 1a, upper half) with $\Delta = 1/2J_{NH}$ (for Fig. 3b), each recorded in 0.75 h. The pulse sequence of Fig. 1b achieves the maximum enhancement of $\sqrt{2}$ (1.41 ± 0.09) for $^{15}N,^{1}H$ spin systems (upper trace in b), but only 0.79 ± 0.16 for $^{13}C,^{1}H$ spin systems (upper trace in a) due to the large number of ^{13}C pulses and the evolution of $^{1}J_{^{13}C,^{13}C}$ coupling. Comparing the sensitivity of the sequence of Fig. 1d for $^{13}C,^{1}H$ and $^{15}N,^{1}H$ correlations (lower traces) with the sequences of Fig. 1a (middle traces), we find that a slight enhancement of 1.07 ± 0.14 (lower trace in a) is obtained for $^{13}C,^{1}H$ correlations, while almost full enhancement of 1.34 ± 0.1 is obtained for the $^{15}N,^{1}H$ correlation (lower trace in b).

propagator of such a pulse pair: $[\exp(i\pi I_x)\ \exp(i\pi S_x), 2\pi J I_z S_z] = 0$; (ii) two delays of equal duration $(\beta/2\pi J_{IS})$, symmetrically about either a 180°(I) or 180°(S) pulse, can be omitted since heteronuclear coupling is refocussed by a single π pulse; and (iii) one 180° pulse can be moved from one side to the other side of a delay $(\beta/2\pi J_{IS})$ during which heteronuclear coupling evolves. At the same time, the direction of evolution of the heteronuclear coupling is inverted due to the following identity: $\exp(i\pi I_x)\ \exp(i\beta I_z S_z) = \exp(-i\beta I_z S_z)\ \exp(i\pi I_x)$. This can be compensated by phase inversion of, for example, the second 90°(S) pulse.

These rules therefore provide a tool to determine the appropriate combinations of gradient signs and pulse phases for the COS-INEPT transfer. Figure 1e explains this point, using the $^{15}N \rightarrow H$ and $^{13}C \rightarrow H$ transfer in the sequence of Fig. 1d as an example.

To compare the performance of the pulse sequences, 2D simultaneous $^{15}N,^{1}H$- and $^{13}C,^{1}H$-HSQC experiments with COS-INEPT were recorded on a 2 mM sample of the $^{13}C,^{15}N$-labeled protein rhodniin with the pulse sequences of Figs. 1b–d (measuring time 1.5 h). These experiments are compared with two separately recorded $^{13}C,^{1}H$-HSQC and $^{15}N,^{1}H$-HSQC experiments with COS-INEPT (pulse sequences of Fig. 1a) that each ran for 0.75 h. An increase in sensitivity of $\sqrt{2}$ for all signals represents the upper limit for the enhancement. The 2D correlation obtained with the pulse sequence of Fig. 1d is shown in Fig. 2. Note the excellent water suppression that allows observation of the H^{α} resonances under the water resonance. If the 1D ^{1}H spectra of the ^{15}N- and ^{13}C-bound protons overlap, the $^{15}N,^{1}H$ and $^{13}C,^{1}H$ correlation spectra can be separated by appropriate phase cycling of the ^{15}N and ^{13}C phases (Sørensen, 1990; Farmer, 1991).

Traces through the spectra recorded with the sequences of Figs. 1b and d are compared to the corresponding reference experiments (Fig. 1a) in Fig. 3. From analysis of 24 N,H and 66 C,H resolved peaks, we conclude that the experiment of Fig. 1b achieves the theoretical sensitivity enhancement of $\sqrt{2}$ for N,H spin systems (1.41 ± 0.09), but yields only 0.79 ± 0.16 for C,H spin systems. This is probably due to the large number of ^{13}C pulses and the evolution of C,C coupling, as explained above. For the experiment of Fig. 1c, which contains more ^{1}H and ^{15}N pulses than the sequence in Fig. 1a, the sensitivity of the simultaneous experiment is decreased for both N,H (0.96 ± 0.08) and C,H spin systems (0.93 ± 0.09). The optimal implementation with respect to evolution of C,C coupling and number of pulses (Fig. 1d) achieves a sensitivity enhancement of 1.34 ± 0.1 for the $^{15}N,^{1}H$ correlation and 1.07 ± 0.14 for the $^{13}C,^{1}H$ correlation. Even for the optimal sequence of Fig. 1d the sensitivity enhancement of the $^{13}C,^{1}H$ correlation in the simultaneous experiment is reduced, due to proton and carbon relaxation during the simultaneous COS-INEPT, which, by contrast to the $^{13}C,^{1}H$-COS-INEPT, must accommodate two $^{1}J_{N,H}$ refocussing periods and is therefore 5 ms longer. The sensitivity of the C,H correlation can be improved by reducing the delay Δ for evolution of the $^{1}J_{N,H}$ coupling from 5.4 to ~4 ms, at the cost of ~9% sensitivity reduction for the N,H correlation. At the same time the sensitivity of the C,H correlation increases by 15% for a ^{13}C T_2 of 20 ms.

In conclusion, we have introduced a simultaneously recorded $^{15}N,^{1}H$- and $^{13}C,^{1}H$-HSQC experiment with COS-INEPT transfers. In the optimal implementation according to the sequence in Fig. 1d, the sensitivity is increased compared to the sequential recording of the experiments and excellent solvent suppression is achieved by the formation of a heteronuclear gradient echo.

Acknowledgements

This work was supported by the 'Fonds der Chemischen Industrie' and the DFG (Gr 1211/6-1). M.M. was supported by a stipend of the 'Fonds der Chemischen Industrie' and J.S. was supported by the DFG through the Graduiertenkolleg 'Chemische und Biologische Synthese von Wirkstoffen' (Gk Eg 53/3-3). We thank Dr. T. Keller, Dr. W. Bermel and Dr. R. Kerssebaum, Bruker Karlsruhe, for continuous support.

References

Boelens, R., Burgering, M., Fogh, R.H. and Kaptein, R. (1994) *J. Biomol. NMR*, **4**, 201–213.

Clore, G.M., Kay, L.E., Bax, A. and Gronenborn, A.M. (1991) *Biochemistry*, **30**, 12–18.

Farmer II, B.T. (1991) *J. Magn. Reson.*, **93**, 635–641.

Farmer II, B.T. and Mueller, L. (1994) *J. Biomol. NMR*, **4**, 673–687.

Hurd, R.E. and John, B.K. (1991) *J. Magn. Reson.*, **91**, 648–653.

Ikura, M., Bax, A., Clore, G.M. and Gronenborn, A.M. (1990) *J. Am. Chem. Soc.*, **112**, 9020–9022.

Kay, L.E., Keifer, P. and Saarinen, T. (1992) *J. Am. Chem. Soc.*, **114**, 10663–10665.

Mariani, M., Tessri, M., Boelens, R., Vis, H. and Kaptein, R. (1994) *J. Magn. Reson. Ser. B*, **104**, 294–297.

Maudsley, A.A., Wokaun, A. and Ernst, R.R. (1978) *Chem. Phys. Lett.*, **55**, 9–14.

Muhandiram, D.R., Xu, G.Y. and Kay, L.E. (1993) *J. Biomol. NMR*, **3**, 463–470.

Muhandiram, D.R. and Kay, L.E. (1994) *J. Magn. Reson. Ser. B*, **103**, 203–216.

Palmer III, A.G., Cavanagh, J., Wright, P.E. and Rance, M. (1991) *J. Magn. Reson.*, **93**, 151–170.

Pascal, S.M., Muhandiram, D.R., Yamazaku, T., Forman-Kay, J.D. and Kay, L.E. (1994) *J. Magn. Reson. Ser. B*, **103**, 197–201.

Schleucher, J., Sattler, M. and Griesinger, C. (1993) *Angew. Chem.*, **105**, 1518–1521; *Angew. Chem., Int. Ed. Engl.*, **32**, 1489–1491.

Schleucher, J., Schwendinger, M., Sattler, M., Schmidt, P., Glaser, S.J., Sørensen, O.W. and Griesinger, C. (1994) *J. Biomol. NMR*, **4**, 301–306.

Sørensen, O.W. (1990) *J. Magn. Reson.*, **89**, 210–216.

Zuiderweg, E.R.P., Petros, A.M., Fesik, S.W. and Olejniczak, E.T. (1991) *J. Am. Chem. Soc.*, **113**, 370–372.